Drone-based 3D Model Reconstruction of Roadways: A Case Study

Kyle Dunphy[1], Vaibhav Makwana[2], Adam Debevc[2], Ted Strazimiri[2], Jinfei Wang[3], Ayan Sadhu[1]

[1] Department of Civil and Environmental Engineering, Faculty of Engineering, Western University London, Ontario, Canada N6A 5B9
[2] Norton Wolf School of Aviation & Aerospace Technology, Fanshawe College, London, Ontario, Canada, N5V 3S4
[3] Department of Geography and Environment, Western University London, Ontario, Canada N6A 5B9
kdunphy2@uwo.ca

Abstract. Structural Health Monitoring (SHM)-based inspections of buildings, roadways, and structures have been conducted manually by qualified individuals. This process often involves the manual vision-based inspection of various elements of the structure to ascertain the level of deterioration associated with the structure. This analysis supports recommendations by engineers as to whether the structure needs to be rehabilitated, redesigned, or replaced as well as an estimate of the appropriate timeline to do so. However, traditional SHM have several limitations due to their manual, human-based nature including high economic costs, logistical constraints (due to limited access to the structure), increased time durations of inspections, and analysis bias due to human involvement in the process. As such, there has been a paradigm shift to involve advanced robotic technology, including unmanned aerial vehicles (UAV), unmanned ground vehicles, cameras, augmented reality, and LiDAR, to help mitigate the costs of conducting SHM inspections while improving their efficiencies. This paper demonstrates the positive benefits of UAV-based inspections for road condition assessment for structural health monitoring. A DJI Matrice 300 Real Time Kinematics (RTK) UAV with a P1 Zenmuse Camera is implemented to conduct a mapping exercise for a 3.5km stretch of asphalt road located outside of London, Ontario, Canada. Best practices for conducting UAV flights for RGB 2D mapping exercises for SHM applications are provided. Furthermore, a description of the drone setup and the parameters chosen for establishing the flight mission path planning and the data collection process is summarized. From the inspection, both a 2D map and a 3D model were developed for the road and right-of-way using commercially available software. Lastly, use cases for the data and models collected and developed through this study are discussed, emphasizing existing SHM inspection frameworks for industry-based practices.

Keywords: Data Visualization, Path Planning, UAV, 3D Model, Asphalt Pavement, Aerial-based Inspections, Remotely Piloted Aircraft System (RPAS)

1 Introduction

In 2021, it was estimated by the Financial Accountability Office of Ontario that 45.3 ± 5.0% of all municipal assets (i.e., roads, bridges, storm, and wastewater systems) were not in a state of good repair with an estimated $52 billion in infrastructure backlog [1]. Structural Health Monitoring (SHM) has been utilized to assess the remaining life cycle capacity of existing infrastructure and determine a suitable rehabilitation plan to improve asset conditions. In the recent decade, through integrating robotic technologies such as UAVs, unmanned rovers, and underwater drones, SHM has seen progress towards more autonomous inspection methods [2-4]. The primary benefit of these devices is their ability to address the common logistical constraints of inspecting structures; both damaged and undamaged, by reaching areas that are inaccessible for traditional manual inspection [5]. In addition, these robotic platforms are often augmented through the use of computer vision techniques such as Machine Learning (ML) algorithms. As a result, the transition from traditional manual inspection to ML-supported UAV inspection allows for the autonomous processing of vision-based data for data classification, segmentation, and quantification in SHM [5].

Predominantly, the majority of research into UAV-based applications for asset inspection as part of an integrated SHM platform has focused on concrete bridges [7-9], and buildings [10-12]. Very few studies have investigated the application of UAVs for damage assessment of asphalt pavement. The improvement of pavement void detection of sinkholes using a deep learning approach trained on infrared images collected by a UAV was investigated [5]. Their proposed EfficientDet algorithm outperformed existing benchmark architectures significantly when pavement defect identification was concerned. However, optimizing flight mission parameters and improving damage geolocalization are needed before this technique can be integrated into an industry-based SHM framework [5]. Comparable limitations were noted in a study that implemented deep learning semantic segmentation networks to locate and estimate the physical parameters of cracks to identify the level of deterioration in the pavement structure [6]. It was noted that environmental factors such as weather, vehicles, and lighting conditions could reduce the overall quality of images collected by the UAV, reducing the accuracy of damage assessments. Limited and imbalanced data may impact the performance of integrated deep learning algorithms for assessing pavement damage. Additionally, concerns about the unauthorized capture of sensitive information or invasion of privacy from aerial imagery may lead to resistance from communities, or legal challenges, potentially hindering the implementation and acceptance of UAV-based SHM frameworks.

Though few studies of UAV applications for pavement monitoring have been investigated, these applications are limited and do not give substantial attention to the data collection process and what factors could impact this process. In this paper, image-based data is collected utilizing a camera mounted on a UAV for a 3.5 km stretch of rural highway outside of London, Ontario. The site parameters and the importance of pavement monitoring from the context of infrastructure maintenance and economic impacts are summarized. The process for preparing and conducting the UAV-based pavement inspection within the framework of Canada's Aviation Regulations (CAR) is

described. Details about the parameters utilized for the UAV's path planning and data collection are provided. The extracted 2D images from the conducted flights are utilized for the creation of a 2D orthomosaic map and 3D model using commercially available software. Finally; the use of this data, within the context of existing SHM frameworks as well as the challenges present in existing UAV-based pavement monitoring techniques, are discussed.

2 Description of the Inspection Site

For this study, a 3.5 km segment of Amiens Rd in Strathroy-Caradoc Township with a speed limit of 80km/h and a traffic count of 50-999 cars/day was chosen, as depicted in Fig. 1. Based on the daily traffic count and the existing speed limit of Amiens Rd, visual inspection is carried out once every 7 days [1]. Pavement monitoring ('Patrolling' based on O. Reg. 23/10, s.3.(1) and O. Reg. 239/02, s.3.(3) [1-2]) and evaluation are essential for ensuring Ontario's roads remain safe. Regular inspection detects potholes, cracks, and shoulder drop-offs; quantifying the extent of deterioration allows public works departments to prioritize required maintenance. Ontario's fundamental, and mandated minimum, maintenance standards ensure that problematic sections are promptly repaired. This robust maintenance strategy is essential for ensuring well-managed roads which form the backbone of an economy that relies on the consistent flow of goods and people between city centers, manufacturing facilities, and end users.

Fig. 1. Satellite image depicting the location of inspection site – Amiens Rd.

3 Proposed Methodology

The following section describes the processes of the pre-flight inspection of UAV devices and related components (tripods, batteries, landing pads, etc.) selected for the visual inspection of Amiens Rd. The equipment assembling process in field applications and the standard safety and flight procedures are summarized. The path planning and flight parameters chosen for the pavement condition assessment are discussed.

3.1 Equipment Setup

For this application, the UAV system selected for the pavement condition assessment of Amiens Rd was a DJI Matrice 300 RTK UAV (the '*drone*' as referenced in the remainder of the paper) with a gimbal-mounted Zenmuse P1 35mm Camera (the '*camera*' as referenced in the remainder of the paper) as shown in Fig. 2. The camera was utilized to capture high-resolution images during the flight. Prior to conducting the flights, all equipment was inspected by the pilot through the use of a "pre-flight checklist" per CAR, SOR/96-433 901.28 and 901.29 [3]. The drone was physically inspected to verify all mechanical and electrical components were in working order and free of visible damage, including the detachable landing gear, frame arms, propellers, motors, and infrared and vision sensing systems. It was ensured that the latest firmware package had been downloaded and installed on both the drone and the Matrice 300 Series DJI Smart Controller Enterprise (the '*controller*' as referenced in the remainder of the paper). The available batteries required for the drone and controller (TB60 and WB37) were inspected for bulging, leakages, and unusual temperatures before being charged and before being flown. A total of 8 TB60 batteries (4 pairs as the drone requires 2 for operation) and 4 WB37s were prepared for this flight.

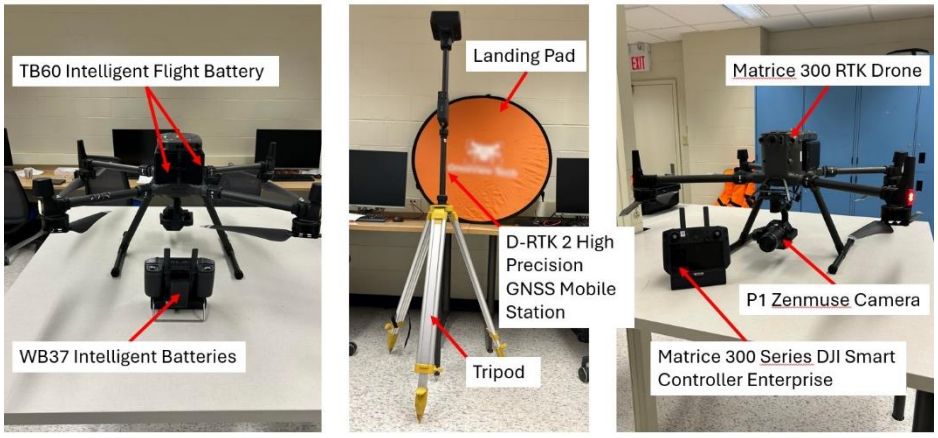

Fig. 2. UAV-based equipment prepared during the pre-flight check.

Before the flight, the pilot conducted a "site survey" following CAR, SOR/96-433 901.27 [3]. The purpose of this site survey was to define the boundaries of the operation,

establish the class of airspace, confirm the legal requirements, and verify the location of hazards at the operation site The proximity of aerodromes, airports, and heliports, as shown in Fig. 3, were recorded. The 3.5km stretch of Amiens Rd invested is in Class G, designated uncontrolled, airspace with a maximum allowable flight altitude of 400 ft above ground level (AGL). Due to the rural location of the highway, as shown in Fig. 1, the most significant hazard was the presence of trees, approximately 60 ft AGL in height; particularly on the south side of Amiens Rd near Glengyle Dr. and north near Ilderton Rd. Additional airborne hazards included power and telephone lines, and domestic and agricultural structures, including houses, barns, and silos Migratory birds were flying in large numbers during the time of the drone flight, which took place in early November 2023. Local landowners, and airfield managers, were contacted and advised of when the flight would be taking place and how long the duration of the flight would be. Landowner permission to take off and land in several locations along the proposed investigation area was granted.

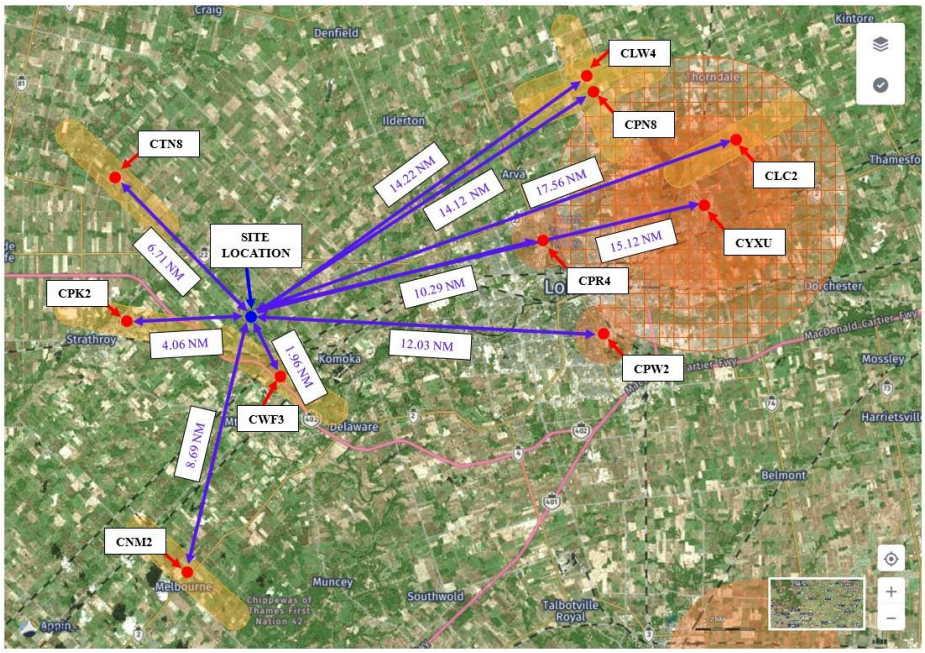

Fig. 3. Site location relative to local heliports, aerodromes, and airports.

3.2 Flight Parameters

A detailed map showing the flight path, take-off/landing areas, and flight area boundaries taken during the pavement condition assessment is depicted in Fig. 4. The approach taken during this study was Visual Line Of Sight (VLOS) (as required by SOR/96-433 901.11 [3]) drone-based data collection. This required our crew to launch and recover the drone multiple times to cover the extent of the inspection area. This

setup requires “visual observers” (SOR/96-433 901.20 [15]) positioned along the roadway (represented by triangular elements in Fig. 4.) to maintain visual contact with the drone throughout its flight, and to communicate details about the status of the operation to the pilot.

Fig. 4. Path planning for Amiens Rd UAV-based inspection.

The inspection of Amiens Rd was segmented into two separate flights in order to maintain VLOS during the planned flights with the assistance of visual observers. The first flight (Flight #1) was planned between approximately 500 m east of Hickory Corners on Amiens Rd to 500 m east of the intersection of Ilderton Rd and Amiens Rd. The second flight (Flight #2) was planned between approximately 300 m west of the intersection of Ilderton Rd and Amiens Rd to 500 m east of Ivan Dr and Amiens Rd. The two flight paths overlapped by a distance of approximately 800 m to ensure enough data was available to integrate each flight in the post-processing stage and to achieve accurate and high-quality results for this boundary region. All path planning was conducted directly in the DJI Pilot 2 app available on the controller. The flight route altitude was selected as 125 ft AGL to achieve an average Ground Sampling Distance (GSD) (the ratio between the distance between two consecutive pixel centers and the real-world measurement on the ground) of 0.48 cm/pixel for both flights. A course angle of flight of 135° was chosen for both flights to ensure the flight path was parallel to the direction of Amiens Rd. This reduced the number of passes required by the drone to capture the full area of the study. Finally, the side and frontal overlap ratios were set to 70% and 80%, respectively, to ensure significant overlap of images recorded by the camera and to prevent the creation of gaps in the final 2D image orthomosaic, particularly at the edges of the images.

4 Data Collection

The D-RTK 2 High Precision GNSS mobile station, drone, camera, controller, and other equipment, including tripod and landing pad, were set up as demonstrated in Fig. 5. The KML flight path files created, as described in Section 3, were uploaded from the controller to the drone to allow for autonomous flight with minimal involvement from the pilot during the two planned flights. A pre-flight briefing was held to discuss the objectives of the flights, the normal operating procedures, emergency procedures, and the duties of the visual observers in accordance with SOR/96-433 901.20, 901.23, and 901.28 [3]. Each visual observer assumed their position, as shown in Fig. 4. before the flight commenced, and radio contact was established to ensure continuous communication between the pilot and the visual observers. During both flights, the D-RTK 2 High Precision GNSS mobile station provided GNSS corrections to resolve time and atmospheric ambiguities with the centimeter-level positioning data of the camera recorded at the time that images were captured. A connection, with an average of 26 satellites, was maintained by the D-RTK 2 High Precision GNSS mobile station to record the GNSS fixed position of each aerial photo throughout both flights. No ground targets or survey benchmarks were measured prior to data acquisition. Based on the chosen area of inspection, as well as the side and frontal overlap ratios and chosen GSD value, a total of 2266 RGB images 8192px in length by 5460px in height with a resolution of 44.73 Megapixels (MP) were captured during both flights. Table 1 summarizes other details regarding each flight; including total travel distance, total inspection area and length, average horizontal speed, flight duration, and the number of images captured during each flight. Once the flights were completed, documentation of the flight including participants, collected data, timing of flights, and the location and duration of the flights was recorded as per SOR/96-433 901.48.

Table 1. Summary of geometric and data parameters for each flight.

Parameter	Flight #1	Flight #2
Total Travel Distance (km)	8.51	7.08
Total Inspection Area (km^2)	0.075	0.061
Total Inspection Length (km)	2.12	1.75
Average Horizontal Speed (km/hr)	18.3	18.3
Flight Duration (mins)	26:06	21:51
GSD (cm/px)	0.48	0.48
Number of Images Captured	1239	1035

Fig. 5. Typical in-field setup of UAV devices and related equipment.

5 Post-Processing of UAV-based Data

Following the completion of the flights, the images were used to create a 2D orthomosaic map and a 3D image model using the commercially available software *DJI Terra*, as shown in Fig. 6. The 2264 captured RGB images, along with the geo-positional data (latitude, longitude, and elevation) collected by the RTK in the form of.NAV files were uploaded to a new visible light reconstruction mission in *DJI Terra* via a MicroSD card that was extracted from the camera post-flight. Table 2 shows the summary of the parameters defined for creating the 2D orthomosaic and 3D models within the software. For aerotriangulation, the standard parameters were selected as the inspection of Amiens Rd does not fall within a "circle" scene, which is considered for the reconstruction of small, primarily vertical objects. Advanced options related to ground control points were not selected as the data collected is georeferenced via the D-RTK 2 mobile station during the flights.

"High resolution" is chosen for the 2D map and 3D model which indicates they will be processed with 100% of the recorded resolution in the field (0.48 cm/px). The horizontal datum of the site (WGS 84 / UTM zone 17N) is specified for both reconstruction scenarios. Post-processing was completed using a LENOVO 30BA00H6US ThinkStation with an NVIDIA RTX A6000 GPU and 48GB RAM. The entire reconstruction process took 12.87 hours with aerotriangulation.. 2D reconstruction and 3D reconstruction took 0.28, 3.30, and 9.28 hours respectively. Based on the aerotriangulation of the georeferenced image data the overall reprojection root mean square error (RMSE) of the images was 0.687px and the georeferencing RMSE of 0.63m based on the analysis conducted in *DJI Terra*. The 2D reconstructed map achieved the desired <0.50 cm/px GSD with a True Digital Orthophoto Map (TDOM) of 0.48 cm/px and a total mapping

coverage of 0.16 km2. The total mapping coverage is slightly larger than the proposed inspection area (0.136 km2) due to the field of view of the camera which captures a larger area which is outside the inspection area defined during the path planning.

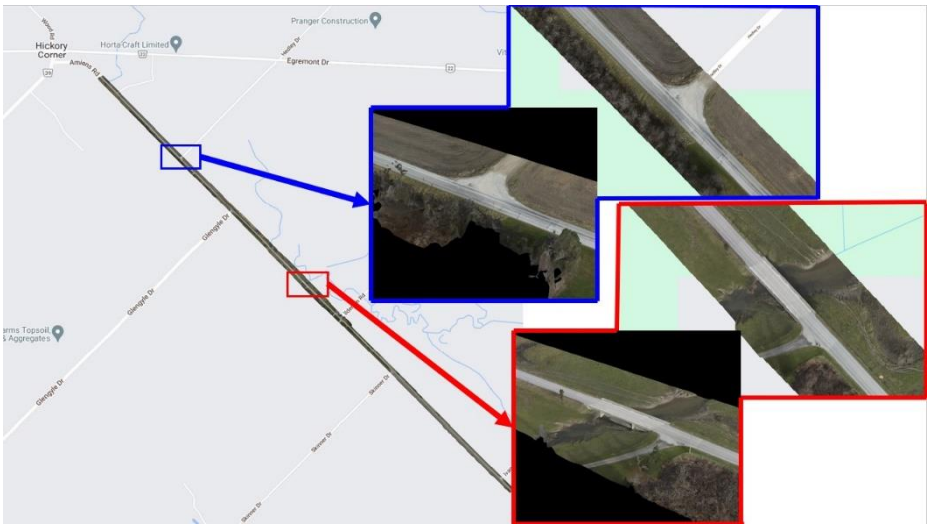

Fig. 6. Example section of the 2D and 3D image model created through DJI Terra.

Table 2. Summary of post-processing parameters used in DJI Terra.

Aerotriangulation	
Scene	Normal
Computation Method	Standalone Computation
2D Visible Light Reconstruction Map	
Resolution	High
Scene	Mapping Scenarios
Computation Method	Standalone Computation
Horizontal Datum Settings	WGS 84/ UTM zone 17N
3D Visible Light Reconstruction Model	
Resolution	High
Scene	Normal
Computation Method	Standalone Computation
Output Format	B3DM
Horizontal Datum Settings	WGS 84/ UTM zone 17N

6 SHM-based Use Cases and Limitations

As mentioned in Section 1, the data collected by UAV is processed by ML algorithms to determine whether damage is present at the image-based or pixel-based level. As the

image data collected through this application is georeferenced through the recording of latitude, longitude, and elevation by the RTK, it is feasible to use the intrinsic and extrinsic properties of the camera to determine the exact location of the damage addressing the concerns of previous studies [5]. However; though a wide region can be inspected and georeferenced through the application of a UAV system, there is a balance that must be considered regarding the compromise between the area of coverage and resolution [3]. For example, the overall quality of the 2D map in this study is excellent, as observed in Fig. 6; however the georeferencing error of 0.63m, though small when compared to the total mapping coverage (0.0004%), may result in significant errors when measuring small quantities which would relate to the condition of the pavement including length and width of cracks as well as the area and depth of potholes. More investigation should be conducted to assess the impact of GSD resolution and reconstruction error on the accuracy of physical quantities extracted from UAV-based imagery.

Fluctuating environmental conditions present a challenge in real-world applications. The uncontrolled variability of factors such as weather, lighting, and the presence of occlusion, such as vehicles and vegetation on the pavement surface may diminish the quality of UAV-based data collection. Although overcast skies are typically a desired phenomenon while collecting aerial images (as there are no shadows cast) they may reduce the ability to discern damage, particularly micro cracks. Factors such as moisture and vegetation have not been investigated, and more studies should be done in a controlled setting to ascertain the impact of environmental factors on data quality. Other mechanical factors, including the speed of the drone, side and frontal overlap ratios, and course angle, should be investigated further to determine their impact on the collection of image-based data from UAVs.

Though 3D modeling is possible with only image data, some features (road profile, depth and breadth of road ditch, and vertical structures such as trees) are of low quality and do not give an accurate representation of profiles observed in the field, as shown in Fig. 6. The use of LiDAR in UAV-based applications would allow for the collection of 3D point clouds which would provide a better representation of the pavement structure. However, the trade-off compared to image-based data is that 3D point cloud data obtained from LiDAR is extensive and requires significant post-processing time compared to image-based models. Furthermore, as most camera and LiDAR-mounted UAV devices save the data to MicroSD cards which have limited space (128GB for this application), storage challenges during inspection may occur. For instance, the 2274 images collected by the camera in this study with the RTK data amounted to 46 GB of collected data, whereas a higher-point-density collection from a Zenmuse L1 LiDAR, (240,000 points/s) would significantly increase the data obtained for the same flight time. Future research should investigate how to extract more accurate 3D information from images obtained from UAV-based applications. With over 300,000 lane kms of road in Ontario, the preferred method to scale data collection beyond a relatively small 3.5 km section of highway are Beyond Visual Line of Sight (BVLOS) flights. There are significant economic benefits to BVLOS drone flights; long-range data-collection flights, without the need to be physically “on-site” with the drone as it captures data, remove the need for large teams of people to be involved.

7 Conclusions

A UAV inspection flight was conducted for a 3.5 km stretch of rural highway (Amiens Rd) by which 2274 RGB 44.73 MP images were collected to assess the overall condition of the pavement. The images were used to create both a 2D map and a 3D model of the site through DJI Terra to assist with the investigation of the pavement quality at this site. A detailed description of the parameters used in the path planning of the flights including GSD, flight elevation, flight area, course angle, side overlap ratio, and frontal overlap ratio was summarized and the error associated with the georeferencing of the data was quantified. Further details were provided about best practices and regulatory guidelines regarding conducting RPAS flights in Canada and how they were implemented in this study. Though this study continued to expand on efforts by previous research concerning UAV-based pavement inspections, there are a few limitations to be considered in future studies. The balance between image resolution and georeferencing error, as it pertains to damage quantification, needs to be further investigated to determine the optimal process for obtaining accurate physical characteristics (crack width, length, angle, etc). The effect of mechanical and environmental factors on the quality of data collected from real-world applications requires deeper exploration. Finally, future research should investigate the feasibility of extracting higher-accuracy 3D data from images collected through UAV applications.

Acknowledgment

The authors would like to thank the Smart Cities and Communities (SCC) laboratory (funded by Western University's Strategic Priority Fund) for providing access to the equipment used in this research. We would like to recognize Good Roads [16] for their financial support and technical contributions to the project. Additionally, financial contributions through student' funding provided by the NSERC CGS-D to the first author are greatly appreciated.

References

1. A Review of Ontario's Municipal Infrastructure and an Assessment of the State of Repair, https://www.fao-on.org/en/Blog/Publications/municipal-infrastructure-2021, last assessed 3/8/2024.
2. Sony, S., Laventure, S., Sadhu, A., A literature review of next-generation smart sensing technology in structural health monitoring. Structural Control and Health Monitoring 26(3), (2019).
3. Sabato, A., Dabetwar, S., Kulkarni, N. N., Fortino, G. Noncontact Sensing Techniques for AI-Aided Structural Health Monitoring: A Systematic Review. IEEE Sensors Journal, 23(5), (2023).
4. Gordan, M., Ismail, Z., Ghaedi, K., Ibrahim, Z., Hashmin, H., Ghayeb, H. H., Talebkhah, M. A Brief Overview and Future Perspective of Unmanned Aerial Systems for In-Service Structural Health Monitoring. Engineering Advances, 1(1), 9 – 15, (2021).

5. Kulkarni, N. N., Raisi, K., Valente, N. A., Benoit, J., Yu, T., Sabato, A. Deep learning augmented infrared thermography for unmanned aerial vehicles structural health monitoring of roadways. Automation in Construction, 148, (2023).
6. Amieghemen, G. E., Sherif, M M. Deep convolutional neural networks ensemble for pavement crack detection using high elevation UAV images. Structure and Infrastructure Engineering, (2023).
7. Yang, J., Bao, Y., Sun, Z., Meng, X. Computer Vision-Based Real-Time Identification for Vehicle Loads for Structural Health Monitoring of Bridges. Sustainability, 16(3), (2024).
8. Perry, B. J., Guo, Y., Atadero, R., van de Lindt, J. W. Streamlined bridge inspection system utilizing unmanned aerial vehicles (UAVs) and machine learning. Measurement, 164, (2020).
9. Ye, X., Ma, S., Liu, Z., Ding, Y., Li, Z., Jin, T. Post-earthquake damage recognition and condition assessment of bridges using UAV integrated with deep learning approach. Structural Control and Health Monitoring, 29(12), (2022).
10. Kim, B., Natarajan, Y., Preethaa, K. R., Song, S., An, J., Mohan, S. Real-time assessment of surface cracks in concrete structures using integrated deep neural networks with autonomous unmanned aerial vehicle. Engineering Applications of Artificial Intelligence, 129, (2024).
11. Akbar, M. A., Qidwai, U., Jahanshahi, M. R. An evaluation of image-based structural health monitoring using integrated unmanned aerial vehicle platform. Structural Control and Health Monitoring, 26(1), (2018).
12. Yu, R., Li, P., Shan, J., Zhu, H. Structural state estimation of earthquake-damaged building structures by using UAV photogrammetry and point cloud segmentation. Measurement, 202, (2022).
13. Municipal Act, 2001, ONTARIO REGULATION 239/02, minimum maintenance standards for municipal highways (Last amendment: 366/18. Legislative History: 288/03, 613/06, 23/10, 47/13, 366/18.) Minimum Maintenance Standards for Municipal Highways, O.Reg. 239/02, s.3(1)., https://www.ontario.ca/laws/regulation/020239, last assessed 3/6/2024.
14. Municipal Act, 2001, ONTARIO REGULATION 239/02, minimum maintenance standards for municipal highways (Last amendment: 366/18. Legislative History: 288/03, 613/06, 23/10, 47/13, 366/18.) Minimum Maintenance Standards for Municipal Highways, O.Reg. 239/02, s.3(1)., https://www.ontario.ca/laws/regulation/r10023, last assessed 3/6/2004.
15. SOR/96-433: Canadian Aviation Regulations, https://laws-lois.justice.gc.ca/PDF/SOR-96-433.pdf, last assessed 3/6/2004.
16. Good Roads, Everything roads since 1894, https://goodroads.ca/, last assessed 3/11/2024.